Materials Today Bio 23 (2023) 100883

Contents lists available at ScienceDirect

Materials Today Bio

journal homepage: www.journals.elsevier.com/materials-today-bio

Controlled electroactive release from solid-state conductive elastomer electrodes

Christopher A.R. Chapman [a,b], Shanila Fernandez-Patel [c], Nusrat Jahan [b], Estelle A. Cuttaz [b], Alexey Novikov [b], Josef A. Goding [b], Rylie A. Green [b,*]

[a] School of Engineering and Materials Science, Queen Mary University of London, Mile End, London, E1 4NS, UK
[b] Department of Bioengineering, Imperial College London, South Kensington, London, SW7 2AZ, UK
[c] Tumour Immunogenomics and Immunosurveillance Laboratory, University College London Cancer Institute, London, UK

ARTICLE INFO

Keywords:
Electrophoretic release
Conductive elastomer
Conducting polymer
Controlled release
Targeted drug delivery

ABSTRACT

This work highlights the development of a conductive elastomer (CE) based electrophoretic platform that enables the transfer of charged molecules from a solid-state CE electrode directly to targeted tissues. Using an elastomer-based electrode containing poly (3,4-ethylenedioxythiophene) nanowires, controlled electrophoretic delivery of methylene blue (MB) and fluorescein (FLSC) was achieved with applied voltage. Electroactive release of positively charged MB and negatively charged FLSC achieved 33.19 ± 6.47 μg release of MB and 22.36 ± 3.05 μg release of FLSC, a 24 and 20-fold increase in comparison to inhibitory voltages over 1 h. Additionally, selective, and sequential release of the two oppositely charged molecules from a single CE device was demonstrated, showing the potential of this device to be used in multi-drug treatments.

1. Introduction

Delivery of pharmaceutical agents to the central nervous system (CNS) is a cornerstone of treatment for many neurological diseases. The treatment in diseases such as Parkinson's, Alzheimer's, or brain cancer relies on the systemic administration of small molecule agents that can cross the blood-brain barrier (BBB) [1]. The two major challenges associated with systemic administration of pharmaceutical agents for diseases in the CNS are off-target effects and poor drug bioavailability [2]. These issues are typically mitigated through balancing the minimum effective dose with the maximum tolerated dose, which is quantified as the therapeutic index [3]. Some treatments such as systemic chemotherapeutic treatments for brain tumors possess a narrow therapeutic index and can cause extreme systemic side effects. Therefore, the development of implanted devices for localized delivery of pharmaceutical agents to the CNS has seen increased clinical attention due to the potential to release high doses of therapeutics directly to the tissue while avoiding off target toxicity commonly associated with systemic therapies [4–8]. Implanted devices have the potential to enable high-dose low-toxicity pharmaceutical delivery in addition to expanding the number of useable pharmaceutical agents by mechanically crossing the BBB. To that end, many hard-to-treat diseases in the CNS stand to benefit greatly from localized high-dose treatments enabled by implanted devices.

Most active devices developed for clinical administration of localized drug delivery have been focused on using pressure to inject liquid drug cocktails into the diseased tissue area (Fig. 1a) [9,10]. The major challenges associated with this method of delivery are the undesirable increases in intracranial pressure and drug reflux along the implant that can arise during administration leading to long administration times and low dose profiles [11]. One potential solution to these challenges is to develop active material platforms that can release controlled amounts without relying on pressure differentials. Bioelectronic devices have enabled the development of technologies capable of performing controlled drug release through the application of an electrical trigger via electrophoresis [12,13]. One successful implementation is the microfluidic ion pump (μFIP) that has been shown to control *in situ* drug delivery of highly concentrated bioactive molecules, such as gamma aminobutyric acid (GABA), to target regions within the brain (Fig. 1b) [14,15]. However, ion pump devices require fluid flow to sustain the concentration gradient across the μFIP, which can pose a risk of uncontrolled drug release upon fluid reservoir breakage.

Solid-state drug delivery completely removes the need for fluid connections at the cost of not having a drug reservoir. Many solid-state

* Corresponding author
E-mail address: rylie.green@imperial.ac.uk (R.A. Green).

https://doi.org/10.1016/j.mtbio.2023.100883
Received 6 September 2023; Received in revised form 14 November 2023; Accepted 22 November 2023
Available online 28 November 2023

polymer drug delivery devices capable of localized controlled release rely on conducting polymers (CPs) such as poly (3,4-ethylenedioxythiphene) (PEDOT), polypyrrole (PPy) and polyaniline (PANI) [12,16]. The properties of CPs enable them to bind charged molecules to their backbones through electrostatic interactions and control their release from the polymer network by changing the reduction-oxidation state of the CP via electrical stimuli [12,16]. CPs also present favorable properties such as high chemical stability, cytocompatibility, and relative low cost of fabrication, which make them ideal for use in implanted devices [16,17]. Most CP-based delivery systems are formed on metallic electrode surfaces using electrodeposition (either potentiostatic or galvanostatic) or through solvent gelation processes (sol-gel). Unfortunately, many of these systems are prone to degradation during release due to poor mechanical stability of the films undergoing repeated reductions-oxidations state changes (Fig. 1c) [18–20]. Polymer composites such as conductive elastomers (CEs) have been designed to help overcome these limitations by combining a percolated network of CPs inside a support network of insulative material, such as an elastomer matrix [18,21–23].

Using CEs as a solid-state electrophoretic release platform has the potential to overcome many limitations of solid CP films alone. First, the elastomeric matrix enables encapsulation of increased amounts of drug in comparison to stand-alone CP films (Fig. 1d). This is a preferable mode of drug storage compared to electropolymerization into a CP film as it protects the CP from degradation caused by reduction and/or oxidation during release. Second, the CP network enables the voltage actuated offloading of charged molecules through a local electric field. In electrophoresis, molecule velocity (v) is governed by electric field strength (E) and the electrophoretic mobility of the molecule (μ_e):

$$v=\mu_e E \quad \text{(Equation 1)}$$

The percolated network of CP inside the CE has the potential to exert a high electric field strength due to the proximity of the entrapped molecules in the elastomeric matrix leading to increased electrophoretic velocity (v) through the polymeric matrix. This means that, depending on molecular charge, an applied electric field can either initiate faster release by increasing electrophoretic velocity away from the polymer network, or inhibit release by increasing electrophoretic velocity towards the polymer network.

These composites have shown long-term stability through processes such as autoclave sterilization seeing little to no change in electrochemical properties after prolonged exposure to traditionally challenging environments for CPs [24]. The ability to be reliably sterilized makes CEs an attractive material platform for clinical use. Ultimately this material offers a middle ground between voltage application to standalone CP film that can cause degradation of the CP film, and the sustained release of μFIPs that require a fluidic connection [25].

In this manuscript, electrophoretic release of small molecules from freestanding CE devices was investigated using a CE composite formed from a polyurethane (PU) matrix, serving as a solid-state polymer reservoir, and PEDOT:dodecyl sulfate (DS) nanowires, providing electrical conductivity. CP conductivity is highly reliant on the presence of dopant molecules [26,27]. Much of the CP work that is done uses commercial dispersions or dry pellets that have high levels of free dopant that confound molecular release. Therefore, in this work a specific dopant-to-CP ratio was achieved using PEDOT:DS nanowires fabricated through a step-by-step doping process [28,29]. DS was chosen as the dopant as it is integral to the formation of the PEDOT nanowires via formation of micelles in which the nanowire polymerization reaction occurs. Residual DS counterions are left after washing which specifically dope the polymerized PEDOT chains. This method minimizes the dopant-CP ionic interactions that may affect quantification of the drug-CP interactions, critical to the drug delivery application. The physical and electrochemical properties of PEDOT:DS nanowire CE has been previously reported over a range of thicknesses (~40 μm–64 μm), with PEDOT:DS nanowire loadings in the range of 10 wt% to 40 wt% showing uniform network formation and improved electrochemical properties with increasing loadings [30]. Additionally, this material has shown excellent biocompatibility in ISO10993 standard indirect contact tests [30,31] alongside successful implementation in *ex vivo* models [24,32].

Due to the nature of this material being freestanding (i.e. not an electrode coating) the PU reservoir can interface with the surrounding reaction environment on both sides of the electrode leading to increased accessible electrochemical surface area. For these mechanistic studies, methylene blue (MB) and fluorescein (FLSC) were used as analogues of

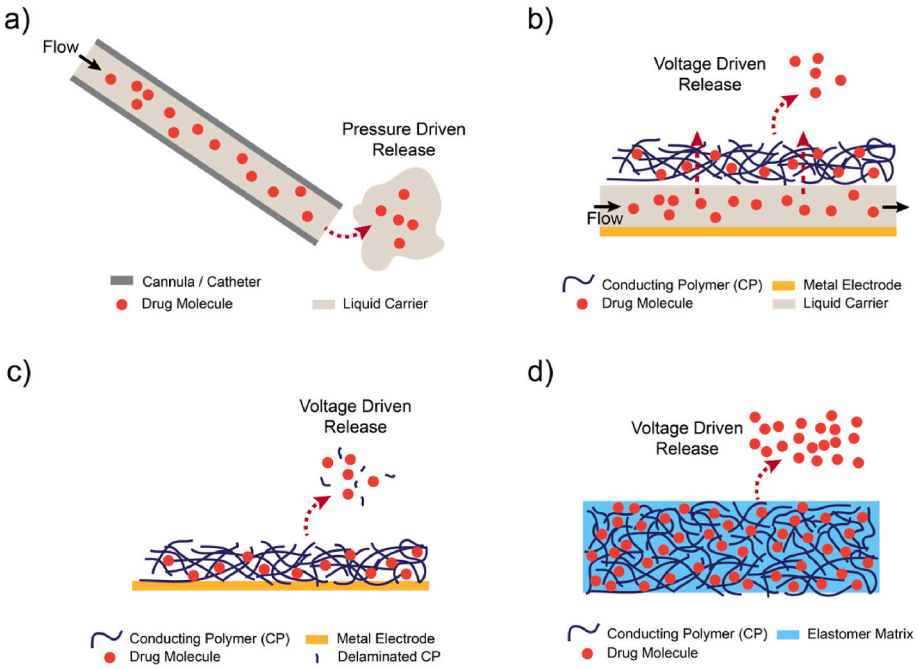

Fig. 1. Schematic of different modes of drug delivery including delivery via liquid injection **(a)**, via electrophoretic ion pump **(b)**, via release from conducting polymer films **(c)**, and via release from conductive elastomers **(d)**.

positively and negatively charged drugs, respectively. Cyclic voltammetry of the drug analogue loaded CE electrodes positively identified target voltage ranges for release of the molecules, and the molecular release profiles across a range of applied voltages and time intervals demonstrated voltage controlled release from the CE material. Optimal voltages for release were then used to achieve sequential release of two oppositely charged molecules from a single device. Ultimately, this work sets a solid foundation for understanding how these complex solid-state polymer systems can be used to facilitate electrophoretic drug release.

2. Results and discussion

2.1. Fabrication of CE-based devices

Fig. 2 outlines the process used for the fabrication of the CE devices. After the drug-loaded CE sheet was cast (Fig. 2a), it was connected to a metallic wire and the wire-bonded region was isolated from the external environment via a silicone capsule (Fig. 2b) to ensure no participation of the metal wire in any electrochemical reactions.

2.2. Cyclic voltammetry

As a preliminary characterization of the entire molecule loaded CE platform, cyclic voltammetry was performed. Cyclic voltammograms (CVs) are essential to provide more details into the chemical events triggered by different voltages. CVs of devices loaded with MB (Fig. 3a) and FLSC (Fig. 3b) were measured and compared to non-loaded CE (Fig. 3c) to investigate the redox properties of each loaded molecule.

At all scan rates, the MB-loaded devices showed that a large irreversible reaction not seen in the unloaded control samples began at voltages around +0.5 V with the peak occurring at voltages greater than +1.2 V. No other clear irreversible reactions occurred at any of the other voltages over all the scan rates. Previous studies on the electropolymerization of MB have found that irreversible MB electrooxidation occurs at a positive threshold potential, leading to polymer formation [33–36]. These studies have shown that this threshold lies between +0.85 V and +0.89 V, at which cation-radical species form, leading to MB electropolymerization [33,36]. The irreversible oxidation of MB seen between +0.5 V and +1.2 V confirms that the low release at high positive voltages is likely due to electropolymerization of the MB molecule during release. MB has been shown to be reversible in the −0.7 V to −0.1 V range, as seen in the MB-loaded devices.

The FLSC-loaded devices showed reversible reactions in the −0.5 V to +0.75 V range with a small irreversible reduction peak at −1.25 V and a small irreversible oxidation peak at +1 V at all scan rates. A similar small irreversible oxidation peak at +1 V was also observed in the control unloaded CE sample therefore it is likely that this is due to changes in the CE and not a redox reaction of the FLSC molecule itself. The small reduction peak at −1.25 V sits in between the −1 V and −2 V voltages later tested for the FLSC-loaded devices and is likely not altering the release appreciably at those voltages.

This data suggests that an optimal release voltage for both MB and FLSC loaded devices exists within the scanned range between −2 V and +2 V. It should be noted that within this voltage window no peaks in current associated with hydrolysis were observed confirming that the CE devices caused no unwanted formation of gases. The peaks present in the CV of the control unloaded CE (Fig. 3c) demonstrated that there is the potential for reduction and oxidation of the PEDOT nanowires in this voltage range. The reduction in current during the slowest (50 mV/s) scan rate for all the CE systems indicated that the electrochemical reactions on CE electrodes were not diffusion limited reactions [37]. Future work investigating the long-term stability of the encapsulated PEDOT network would need to be compared to stand-alone CP films to support the stability benefit of the CE platform.

2.3. Optimization of release voltages

To identify the optimal release voltages within the −2 V to +2 V window for both the positively charged MB and negatively charged FLSC, a range of voltages was used to trigger active release over an hour-long duration (Fig. 4a).

2.3.1. Methylene blue loaded devices

A passive release control with 0 V applied to the device released 20.58 ± 3.49 μg of MB within the hour duration. Significantly increased release of MB in comparison to passive release (0 V) was obtained at a potential of +0.5 V with an amount of 33.19 ± 6.47 μg (Fig. 4b). This accounted for a total device release of 21.4 % of the loaded amount over the 1 h tested. In addition to significant active release, significant inhibition of MB release was successfully demonstrated at negative voltages. The lowest MB release was 1.522 ± 1.26 μg at −2 V, which was statistically significant compared to the release at +0.5 V and passive release (0 V). A significant decrease of MB release was seen at higher positive voltages (+1 V, +2 V) in comparison to passive release. This supports the redox peaks seen during cyclic voltammetry of the MB devices (Fig. 3a) being from electropolymerization of the molecule.

2.3.2. Fluorescein loaded devices

A passive release control with 0 V applied to the device released 5.73 ± 0.99 μg of FLSC within the hour duration. Significantly increased release of FLSC in comparison to passive release (0 V) was obtained at potentials of −0.5 V, −1 V, and −2 V (Fig. 4c). The maximal FLSC release was obtained at −2 V at an amount of 22.36 ± 3.05 μg, a 3.9-fold higher release than passive release. This accounted for a total device release of 7.98 % of the loaded amount over the 1 h tested. Since −2 V was identified as the maximal release voltage, an additional test at −3 V was conducted to investigate if −2 V was a local maximum. The released amount at −3 V decreased significantly from −2 V suggesting that −2 V is an optimal release range for FLSC. Significant inhibition of FLSC release was also achieved at +2 V (1.669 ± 0.51 μg), with an

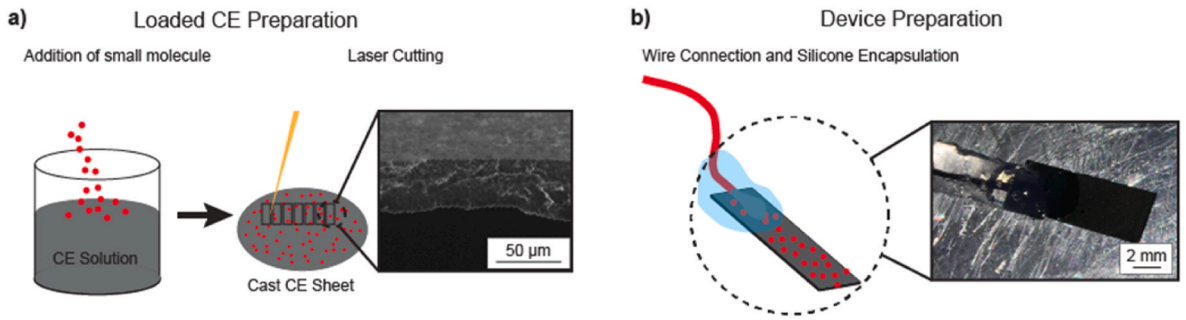

Fig. 2. Fabrication steps of the CE-based electrophoretic release device: a) fabricating and laser cutting molecule-loaded CE, b) connecting wire to molecule-loaded CE sheet and sealing with silicone.

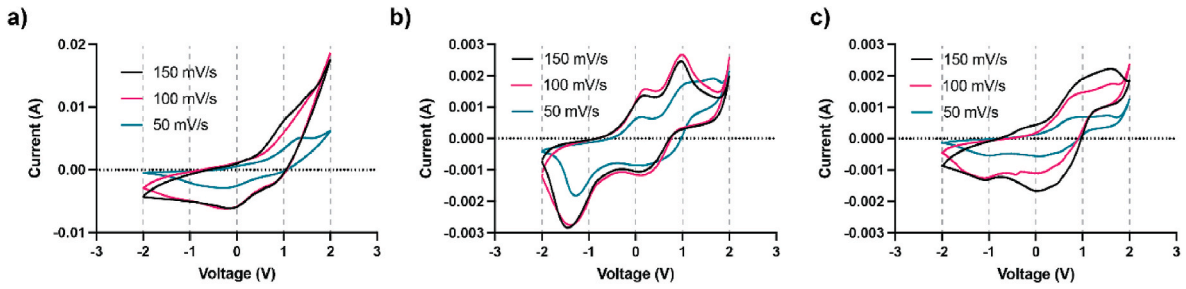

Fig. 3. Cyclic voltammograms of CEs with MB/FLSC/and unloaded. a) MB loaded CE, b) FLSC loaded CE, c) control unloaded CE. All measurements taken in 1 M PBS. Single scan of 11 shown. A total of three devices (n = 3) was used for each scan rate (9 devices per molecule).

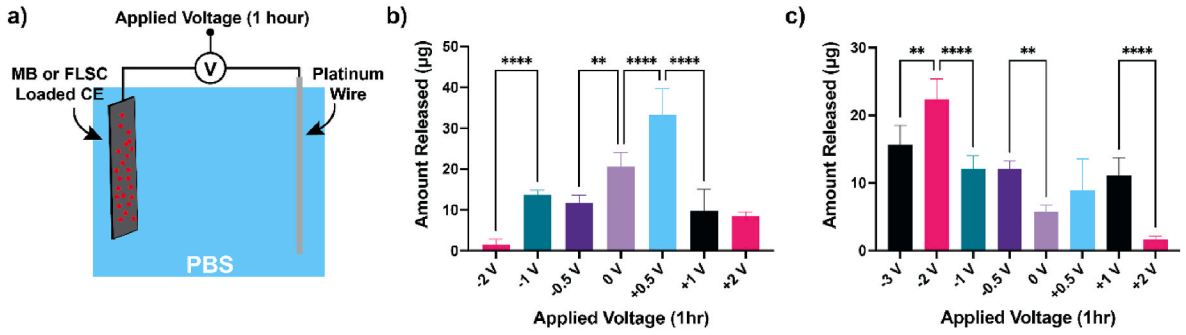

Fig. 4. a) Schematic of experimental protocol. **b)** MB release from PEDOT:DS nanowire CE-based platforms stimulated at the indicated voltage for 1 h. **c)** FLSC release from PEDOT:DS nanowire CE-based platforms stimulated at the indicated voltage for 1 h. One-way ANOVA with Tukey's post-hoc analysis, significance designated by (* = $p < 0.05$, ** = $p < 0.01$, *** = $p < 0.005$, **** = $p < 0.001$). Five devices (n = 5) were tested per voltage for both MB and FLSC devices.

approximately 3.75-fold reduction in released amount in comparison to passive (0 V) release.

Interestingly, the MB and FLSC loaded devices presented drastically different maximal release during passive release conditions. The higher amount for MB is likely due to the molecule possessing the same charge as the positively charged PEDOT network and the small amount of mobile dopant to retain it in the PEDOT:DS nanowire system. Conversely the lower passive release for the FLSC devices is likely due to some interactions between the negatively charged FLSC molecule and the positively charged PEDOT network. The maximal active release amount for both MB and FLSC were relatively low as a percentage of the total amount loaded pre-release (21.4 % and 7.98 % respectively). One potential explanation for these values is that the interaction between the PU and the reaction environment is too slow to enable adequate electrolyte flow out of the PU matrix. This could be due to the lack of swelling for the type of PU utilized for this study (Pellethane 2363-80AE), which swells less than other more hydrophilic PUs [38]. Although use of a hydrophilic PU would likely improve maximal release amount for this system, it is likely that the increase in swelling and porosity would increase the passive release further from the values seen in this study. Inhibitory voltages were able to successfully restrict release over the hour-long period. However, if opposite voltages were to be used to prevent passive release, processes such as unwanted electropolymerization, which limit the platform's capability of dual drug delivery, would need to be addressed. To evaluate this method of passive release prevention, release reversibility was studied.

2.4. Release reversibility

If voltage inhibition of release is to be used as a mechanism to stop unwanted passive release in these devices, the impact on subsequent active release must be investigated. Release reversibility was measured by first inhibiting the release at each of the voltages shown to reduce the release amount below passive release for 1 h. These voltages were −2 V, −1 V, and −0.5 V for MB and +2 V for FLSC respectively (Fig. 4). After 1 h of release inhibition the optimal active release voltage was applied for an additional hour and the total amount released was measured (Fig. 5a).

For MB-loaded devices, after an initial 1-h inhibition at −2 V, active release at +0.5 V for a second hour achieved a total release of 14.62 µg, proving switchable release of MB is possible via electrical stimulation and that the application of a −2 V inhibitory voltage can be used to prevent MB passive release (Fig. 5b). Although successful, the post-release inhibition amount was found to be 44 % of the previously identified maximum release amount (33.19 µg) for the MB devices. MB-loaded devices with initial inhibitory voltages of −1 V and −0.5 V also successfully released MB after an active voltage application, however, due to the high release during the inhibitory stimulation, these voltages would not be adequate for the development of a controlled drug delivery mechanism.

FLSC-loaded devices were initially inhibited at the positive voltage +2 V which led to minimal release of FLSC from the device. After 1 h of inhibitory voltage application, FLSC was actively released from the devices at the previously identified optimal voltage (−2 V) for 1 h. Devices that were subjected to a +2 V inhibitory voltage achieved a total release of 11.88 µg, after active release at −2 V (Fig. 5c). Similarly, although the release was successfully switched between inhibition and active release only 53 % of the previously identified optimal FLSC release (22.36 µg) was successfully released.

Although the ranges of optimal release voltages were verified by the CVs, the cause of the drop in active release amount after switching from an inhibitory voltage is still unclear. It is possible that this phenomenon is not caused by a redox reaction, but rather the inhibitory voltage further attracting the charged molecule deeper within the bulk of the polymer matrix. This will hinder the pathway for molecule movement out of the polymer, causing a lower rate of active diffusion and hence reduced amount released [39,40]. Further studies investigating molecule mobility through the CE matrix could elucidate this complex interaction between the CP, molecule, and elastomeric matrix, with a focus on studying the impact of an inhibitory voltage prior to active

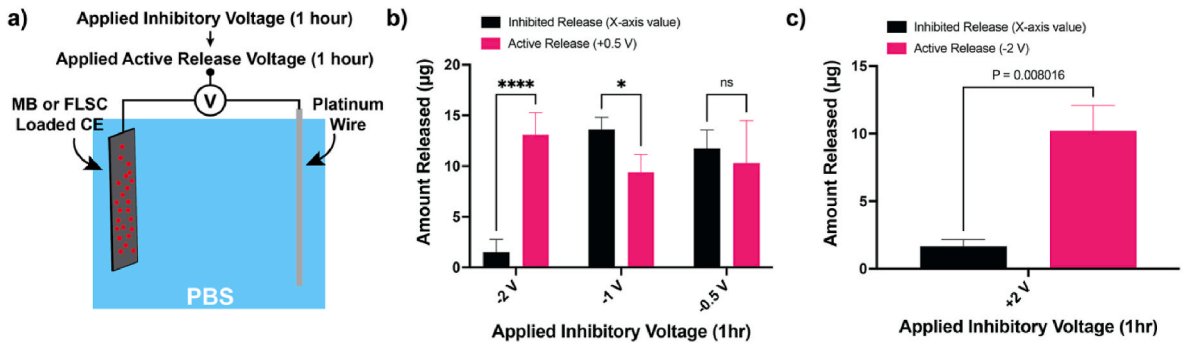

Fig. 5. a) Schematic of experimental protocol. **b)** MB release from devices stimulated at +0.5 V for 1 h, after stimulation at the indicated inhibiting voltage for 1 h. **c)** FLSC release from devices stimulated at −2 V for 1 h, after stimulation at the indicated voltage for 1 h. Two-way ANOVA with Bonferroni post-hoc comparison, significance designated by (* = $p < 0.05$, ** = $p < 0.01$, *** = $p < 0.005$, **** = $p < 0.001$). Five devices (n = 5) were tested per voltage for both MB and FLSC devices.

release of the molecule.

2.5. Release profiles

The electrophoretic release of MB and FLSC was also measured over time to assess the overall release profile from the device (Fig. 6). Both molecules were released over an hour-long period at the previously identified optimal release voltages. As seen in Fig. 6, application of the inhibitory voltages (−2 V for MB, and +2 V for FLSC) effectively minimized release for the entire hour-long period of release. Active release for both molecules (+0.5 V for MB, and −2 V for FLSC) was consistent with the results obtained previously (Fig. 3). A 24-fold increase in release for the MB and 20-fold increase for the FLSC were seen in comparison to the inhibited release. Release profiles differed between the two molecules with both the active and passive release of MB having an initial burst release at the 1-min timepoint whereas active and passive release of FLSC followed a more linear trend. It is likely due to the relatively weak interactions between the MB molecule and the negatively charged dopant in comparison to the stronger interactions between FLSC and the positively charged PEDOT polymer. Molecular flux, defined as the number of molecules crossing a surface in a single direction over time, can also be inferred from this data due to the consistency in device geometry used for the release [41]. Outside of the initial burst release molecular flux for MB is not altered by the applied voltage whereas the rate of FLSC release is increased over the full 1-h timepoint. This further suggests that there are distinct differences in the interactions between the PEDOT nanowires and the molecules being released depending on their charge.

Although the high passive release of MB is not desirable, the interactions between the molecule and the CP/dopant complex have potential to be further tailored to improve the resulting passive release. By altering dopant size or dopant charge density with a molecule such as polystyrene sulfonate (PSS), the interactions between the positively charged molecules can be altered to reduce passive release. However, the reduction in passive diffusion would likely come at the cost of decreased maximum release amount or an increase in total release time due to hindrance of molecular diffusion.

Further investigation of the release reversibility demonstrated the potential for both MB and FLSC-loaded devices to achieve fully voltage-regulated control of release. Fig. 7 shows release profiles of 1 h release inhibition followed by active release for 2 h of both MB and FLSC-loaded devices. Both molecules were successfully released on demand at the 1-h mark (between red and green highlight) by switching the voltage applied to the device from inhibitory to active release. After 2 h of release neither device reached a true plateau, however the release from both devices was minimal between the 1-h and 2-h time points. Interestingly, release kinetics during the first minutes after switching from voltage inhibition to active release are affected in the FLSC-loaded devices. This is seen as a lag in release speed after switching (Fig. 7b) and may be due to inhibitory voltages further impacting the molecules into the elastomeric matrix as suggested in Section 2.3.

The ability for each device to successfully inhibit release of the loaded molecule and then trigger a release on demand is a useful function when considering the device as a method for releasing a single therapeutic on demand. However, in many drug delivery applications it is often desirable to give multiple agents sequentially.

2.6. Sequential release

The potential for the sequential release of two different molecules from the same device using opposing voltages was investigated using a single device fabricated from MB and FLSC-loaded CE sheets bonded

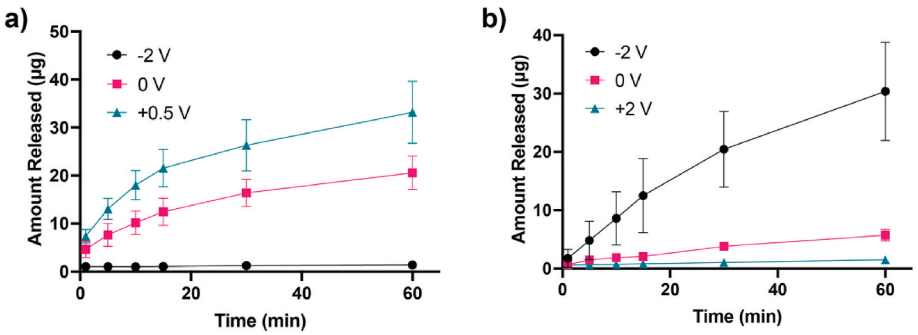

Fig. 6. a) MB release from PEDOT:DS nanowire CE-based platforms stimulated at −2 V, 0 V, or +0.5 V for 1 h. **b)** FLSC release from PEDOT:DS nanowire CE platforms stimulated at −2 V, 0 V, or +2 V for 1 h. Five devices (n = 5) were tested per voltage for both MB and FLSC-loaded devices. Samples were taken and measured at timepoints of 5, 10, 15, 30, and 60 min.

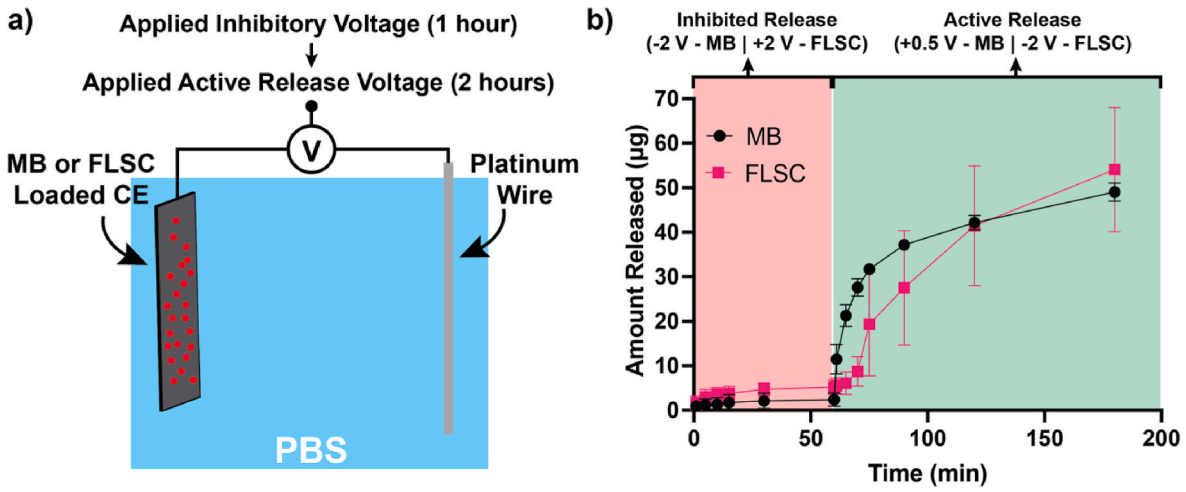

Fig. 7. **a)** Schematic of experimental protocol. Devices were held at an inhibitory voltage (-2V for MB, +2 V for FLSC) for 1-h with a subsequent 2-h long release at an active release voltage (+0.5 V for MB, −2 V for FLSC). **b)** Release profiles of MB and FLSC loaded devices. Red highlighted area denotes time release was inhibited; green highlighted area denotes time release was active. Five devices (n = 5) were tested for both MB and FLSC-loaded devices. Samples were taken and measured at timepoints of 5, 10, 15, 30, and 60 min for the inhibited release and at timepoints of 5, 10, 15, 30, 60, and 120 min for the active release.

together with the same control wire (Fig. 8a). Release of FLSC was successfully achieved with a driving voltage of −2 V applied to the device, which simultaneously served to inhibit MB release. After 1-h of voltage application 30.38 ± 8.45 µg of FLSC had been released compared to only 3.36 ± 3.46 µg of MB. After 1-h at −2 V the applied voltage was switched to +0.5 V to a regime where MB would be actively released. After the second hour of release the amount of MB increased to 72.5 ± 11.28 µg, a 21.6-fold increase, and the amount of FLSC increased to 43.34 ± 10.93 µg, a 1.4-fold increase (Fig. 8b). Although the FLSC release decreased during the second hour compared to the expected 2-h release value seen in Fig. 7, the application of +0.5 V to the device did not fully inhibit the release of FLSC as is seen in the quantification of the discrete release amounts (Fig. 8c). Additionally, the negative impact of the inhibitory voltage on the MB-loaded CE seen previously (Fig. 7) was not seen in the sequential release set-up. This is potentially due to the presence of a second CE sheet (Fig. 8a) creating an additional current pathway with increased current flux throughout the application of the inhibitory voltage, thus directly affecting the MB molecule during inhibition. Future work is underway combining both molecules into a single sheet. Although this will undoubtedly shed light on this phenomenon, it was avoided in this instance as it has the potential to introduce further molecular interactions between the released molecules.

One of the major challenges associated with controlled release is overcoming the passive release associated with bulk diffusion of the molecule away from the device. Here, an inhibiting voltage was successfully used to stop this diffusion, however from a power consumption standpoint it is not ideal to constantly apply a voltage to the electrode over the implanted device lifetime. Future work on this device aims to prevent passive release through modifying components of the carrier polymer matrix. One potential method would be to alter how the drug is carried in the polymer matrix. Polymer carriers such as nanoparticles are attractive candidates as drug delivery system with enhanced bioavailability and high capacity for functionalization [42,43]. By using charged nanoparticles, it may be possible to inhibit passive release due to the intrinsic charge properties of the polymer matrix while maintaining electrophoresis control over the release [44]. Additionally, other methods for preventing passive release, such as the use of surface coatings [45–47] or the modification of the polymer matrix of the CE [44,48,49] could be investigated. Another potential challenge for molecular delivery using CEs is that the charged dopant is not covalently linked to the CP component. This means that there is potential for dopant flux out of the material during voltage application, leading to undesirable release of potentially toxic chemical dopants [39,40]. A method to prevent this would be to utilize self-doping CP systems [50] which would remove dopant mobility from the system entirely. Alternatively, further removal of excess dopant from the system before loading the CE could aid in reducing any potential dopant release. Specifically doping the PEDOT matrix for each releasing agent, although labor intensive, could have profound effects on release efficacy from a

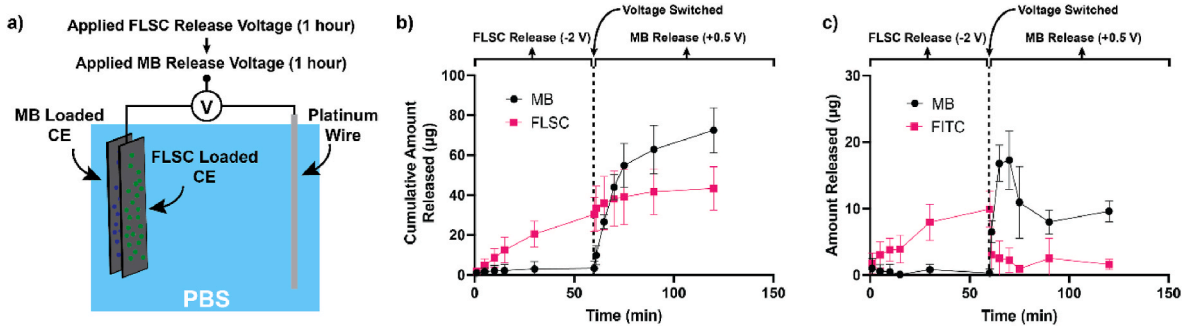

Fig. 8. **a)** Schematic of experimental protocol. FLSC was actively released for the first hour at −2 V (while inhibiting MB release) and MB was actively released for the second hour at +0.5 V (while inhibiting FLSC release). **b)** Cumulative release profiles of MB and FLSC dual release from a CE-based device containing both molecules (n = 4). Samples were taken and measured at timepoints of 5, 10, 15, 30, and 60 min for both sequential releases. **c)** Discrete released profile of MB and FLSC dual release from a CE-based device containing both molecules (n = 4).

dual release system. Further analysis of the eluent post-release using analytical methods such as liquid chromatography-mass spectrometry (LCMS) would add significantly to the understanding of the role dopant mobility plays in this system. Accessible electrochemical and real surface area also plays an important part in the drug release kinetics from composite materials such as the CE explored in this work. In depth analysis of the material roughness and real surface area could also open new avenues to improve the control over the molecular release from this material. Although this manuscript focused on 1 h of release to target an acute release profile, further studies investigating increasing the release time of the CE platform may also shed light on the long-term dynamics of the molecular release from the CE. Additionally, other modes of electrically triggered release such as electrochemical actuation of the PEDOT nanowires could be employed to improve release rate from the electrodes [25].

FLSC and MB are commonly used as drug models because their fluorescent properties facilitate monitoring and measurements of their release, however these results demonstrate that molecular release kinetics from this device are strongly dependent on molecular and structural properties. Therefore, drug analogues are unlikely to be sufficiently accurate models for drugs of interest such as chemotherapeutic agents. Whilst MB undergoes electropolymerization upon stimulation at high positive potentials [33,35,36], other molecules will likely experience other reactions. For example, studies have found that a surface-bound complexation of cisplatin, a positively charged chemotherapeutic drug, can be reduced electrochemically to form Pt nanoparticles on a gold electrode upon negative potential scanning [51]. If used in a dual drug delivery CE-based platform, cisplatin could undergo structural changes upon stimulation at a negative voltage, affecting its release and bioactivity [52]. Another example is doxorubicin, a positively charged anticancer drug. Whilst some CV studies have shown it only presents one reversible two-electron reduction [53,54], others have found a second reversible or irreversible peak by slightly varying the scan rate and pH conditions [54–56]. Therefore, to fully understand the behavior of a drug under electrical stimulation in a CE-based platform, detailed studies must be carried out on direct drug analogues possessing sufficient functional and structural similarities [57].

Although the CE system proposed in this study shows significant promise for the controlled release of small molecules using electrophoresis, both the strengths and limitations of the material as a drug delivery device must be considered. One of the major benefits of this material is the ability to fine tune both the CP and elastomer properties to achieve the desired release profiles. Future work will focus on highlighting the important interactions between the CE components and drug molecules in this complex material. These studies will help to address the major limitations of molecular release time due, in part, to limited swelling of the elastomeric matrix. Another benefit of this material is the ease of processing and scalability of manufacturing. Since this material relies solely on a volume determined casting process with constant loadings of PEDOT nanowires, it is extremely flexible for mass production. One limitation of the current processing method is that the solvents needed to disperse both PU and PEDOT nanowires during manufacturing limit the types of molecules amenable to this process. In the future, use of functionalized PUs could help mitigate this limitation through enabling the use of water as a common solvent [58].

Overall, this work has demonstrated that the CEs can provide a middle ground between nanogram release from typical drug eluting electrodes [59] and the milligram delivery associated with direct injection [8]. Although the current data suggests delivery over an acute time period would be the most successful, translation into an implantable cartridge delivery device that could be loaded on an outpatient basis could provide the chronic delivery necessary for treatment of many hard-to-treat diseases. Further work exploring the vast parameter space associated with this device is currently underway. Of particular interest is elucidating the effect of molecular loading amount on the voltage mediated release kinetics and transitioning to use with relevant charged small molecule drugs such as doxorubicin or dexamethasone.

3. Conclusions

The controlled electrophoretic release of pharmaceutical agents directly into the CNS is a promising methodology for significantly improving the local bioavailability of the desired therapeutic. This work has highlighted the development of a solid-state electrophoretic releasing polymer system and its use as a highly controllable release platform capable of actively releasing both positively and negatively charged molecules. This foundational work provides an initial understanding of the mechanisms behind molecular release in a CE-based electrophoretic device. Using these results, future work optimizing the release of charged pharmaceutical agents can be investigated more successfully. Ultimately this device presents a potential paradigm shift for the treatment of CNS diseases to significantly improve clinical prognosis in these patients.

4. Material and methods

4.1. Fabrication of drug analogue-loaded conductive elastomer sheets

PEDOT nanowires doped with dodecyl sulfate (PEDOT:DS) were fabricated based on previously reported protocols [60,61]. Briefly, 90 mMol sodium dodecyl sulfate (SDS) (Sigma) was dissolved in 300 mL of deionized water (DI) and stirred at 500 rpm for 15 min. 7 mL of 48.99 mMol iron chloride (III) solution was then added and stirred at 500 rpm for 1 h at 50 °C in an oil bath. Whilst stirring, 21 mMol of 3,4-ethylenedioxythiophene monomer (EDOT) (Sigma) was slowly injected. The solution was left at 50 °C for 5 h 30 min to polymerize. The resultant solution was washed by centrifuging to remove excess molecules dopant and iron chloride. The resultant nanowire material was dispersed in 250 mL of methanol and 15 mL of the obtained solution was vacuum filtered onto a 0.1 μm polyvinylidene fluoride (PVDF) filter (Durapore, Merck) membrane to produce a PEDOT:DS nanowire sheet. The nanowire sheets were left to dry at room temperature overnight. PEDOT:DS nanowire CEs were fabricated based on a modified version of a previously reported protocol [62]. Briefly, polyurethane (PU) (Pellethane 2363-80AE Polyurethane Elastomer, Ether Based, Velox GmbH) was dissolved in dimethylacetamide (DMAC) (Sigma) for 24 h at 60 °C stirring constantly at 300 rpm. Then, lithium perchlorate salt was added and allowed to stir at 60 °C for an additional 12 h. Here, dried PEDOT:DS nanowire sheets were then sonicated in a DMAC/PU mixture before being added to a larger solution resulting in a 25 wt% loading of PEDOT:DS nanowires. The drug analogue, either methylene blue (MB) (Sigma) or fluorescein (FLSC) (Sigma) was loaded into the 25 wt% PEDOT:DS nanowire CE solutions by adding the analogue to the initial dispersion of PEDOT:DS nanowire and PU and stirring for 24 h. The ratios of drug analogue to PU used in the CE sheets were 0.18:1 for MB and 0.1:1 for FLSC. More exactly, a single sheet contained 0.3 g of PU, and 0.054 g of MB or 0.03 g of FLSC. This led to device specific loadings of approximately 280 μg for the MB-loaded devices and 155 μg for the FLSC-loaded devices. The drug-loaded CE solution was then cast into sheets and dried in the vacuum oven for 36 h at 65 °C to form the CE sheets. Once cast, the sheets were laser cut into 10 mm × 3 mm sheets using a 1064 nm MOPA fiber laser (Lotus Laser Systems). According to previously published work, unloaded PEDOT:DS nanowire CE sheets exhibited conductivities in the range of 50 S/cm [62].

4.2. Device connection and silicone encapsulation

The 10 mm × 3 mm drug-loaded PEDOT:DS nanowire CE sheets were connected to a 7 cm long section of AWG30 silver plated copper wires (RS Components). The CE-wire bonding area was then encapsulated in 2 layers of medical grade silicone (NuSil MED4-4220) to ensure that, whilst the device is in use, the external saline environment does not

penetrate through the CE and interact with any metallic surfaces.

4.3. Electrochemical experiments

All electrochemical experiments were performed at room temperature in a static saline environment to create a controlled reaction environment.

4.3.1. Cyclic voltammetry of devices

All CV measurements were done using a three-electrode set-up with the CE device as the working electrode, a platinum wire as the counter electrode, and a leakless silver/silver chloride electrode as the reference. Devices were immersed in 1 mL of 1 M phosphate buffered saline (PBS) and CVs were measured with a potentiostat (Autolab) at scan rates of 150, 100, and 50 mV/s. Fresh PBS was used for each measurement to ensure that no concentration dependent mechanisms had an impact on the measurements.

4.3.2. Voltage application for release

All voltage application for release was done using a two-electrode set-up with the CE device as the working electrode and a platinum wire as both the counter and reference electrode. Devices were immersed into 1 mL of PBS and a constant voltage was applied using a potentiostat (Autolab).

4.4. Fluorescence quantification

Fluorescence measurements of the released samples were made using a NanoDrop 3300 fluorospectrometer. MB fluorescence was measured at 686 nm, and FLSC fluorescence was measured at 515 nm. Average results of fluorescence of the PBS solution after electrical stimulation were used to quantify the analogue release. For FLSC, 10 μL of the PBS containing drug analogue were diluted into 990 μL of pure PBS to obtain fluorescence levels detectable by the fluorospectrometer. This was only necessary for FLSC due to its high fluorescence intensity. Five separate 2 μL droplet-measurements were taken per sample to estimate an average fluorescence per device. Approximate quantities of drug analogue release were inferred from the fluorescence measurements by using a standard curve measured on the same fluorospectrometer.

4.5. Statistical analysis

Data analysis was done using Microsoft Excel and Python software (pandas package). Statistical analysis was performed using Graphpad Prism and the specific statistical tests for each figure are noted in the figure caption. The data is reported as mean ± standard deviation unless otherwise noted in the figure caption. Sample sizes varied from three (3) to five (5) depending on the experiment, therefore exact sample sizes are noted in the figure captions for each experiment.

Author contributions

C.A.R.C. wrote the manuscript and led experimental direction of the project. S.F. collected data for preliminary release experiments and provided writing for the manuscript. N.J. collected data for cyclic voltammetry and sequential release experiments. E.A.C. fabricated the conductive elastomers used in the experiments. A.N. performed scanning electron microscopy of the conductive elastomers. J.A.G. provided insight into experimental design. R.A.G. provided funding, experimental design, overarching project leadership and editing for the final manuscript.

Declaration of competing interest

The authors declare the following financial interests/personal relationships which may be considered as potential competing interests: Rylie Green reports financial support was provided by Engineering and Physical Sciences Research Council. Christopher Chapman reports financial support was provided by Rosetrees Trust.

Data availability

Data will be made available on request.

Acknowledgements

The authors acknowledge funding from the Engineering and Physical Sciences Research Council (EPSRC) as part of an IRC grant on Hard-to-treat cancers [EP/S009000/1] and the Healthcare Technologies Challenge Awards (HTCA) grant. Additionally, C. A. R. Chapman acknowledges funding from a Rosetrees Trust Enterprise Fellowship [EF2020 \100033].

References

[1] John Kelly, Principles of CNS Drug Development: from Test Tube to Clinic and beyond, 2009.
[2] Q. He, J. Liu, J. Liang, X. Liu, W. Li, Z. Liu, Z. Ding, D. Tuo, Cells 7 (2018) 24.
[3] J. Tamargo, J.-Y. le Heuzey, P. Mabo, Eur. J. Clin. Pharmacol. 71 (2015) 549.
[4] M.F. Lam, M.G. Thomas, C.R.P. Lind, J. Clin. Neurosci. 18 (2011) 1163.
[5] M.A. Vogelbaum, M.K. Aghi, Neuro Oncol. 17 (2015), https://doi.org/10.1093/neuonc/nou354.
[6] N.U. Barua, S.P. Lowis, M. Woolley, S. O'Sullivan, R. Harrison, S.S. Gill, Acta Neurochir. 155 (2013), https://doi.org/10.1007/s00701-013-1700-6.
[7] A. Jahangiri, A.T. Chin, P.M. Flanigan, R. Chen, K. Bankiewicz, M.K. Aghi, J. Neurosurg. 126 (2017), https://doi.org/10.3171/2016.1.JNS151591.
[8] E. Szychot, D. Walker, P. Collins, H. Hyare, A. Shankar, A. Bienemann, M. Hollingworth, S. Gill, Int. J. Clin. Oncol. (2021) 26, https://doi.org/10.1007/s10147-020-01853-0.
[9] A.M. Mehta, A.M. Sonabend, J.N. Bruce, Neurotherapeutics 14 (2017), https://doi.org/10.1007/s13311-017-0520-4.
[10] O. Lewis, M. Woolley, D. Johnson, A. Rosser, N.U. Barua, A.S. Bienemann, S.S. Gill, S. Evans, J. Neurosci. Methods 259 (2016), https://doi.org/10.1016/j.jneumeth.2015.11.008.
[11] N.U. Barua, S.S. Gill, S. Love, Brain Pathol. 24 (2014) 117.
[12] C.A.R. Chapman, E.A. Cuttaz, J.A. Goding, R.A. Green, Appl. Phys. Lett. 116 (2020), 010501.
[13] S. Löffler, B. Libberton, A. Richter-Dahlfors, Electronics (Switzerland) 4 (2015) 879.
[14] C.M. Proctor, A. Slézia, A. Kaszas, A. Ghestem, I. del Agua, A.M. Pappa, C. Bernard, A. Williamson, G.G. Malliaras, Sci. Adv. 4 (2018) 1.
[15] L. Waldherr, M. Seitanidou, M. Jakešová, V. Handl, S. Honeder, M. Nowakowska, T. Tomin, M. Karami Rad, T. Schmidt, J. Distl, et al., Adv. Mater. Technol. (2021) 6, https://doi.org/10.1002/admt.202001302.
[16] Y. Park, J. Jung, M. Chang, Appl. Sci. 9 (2019) 1070.
[17] R.A. Green, N.H. Lovell, G.G. Wallace, L.A. Poole-Warren, Biomaterials 29 (2008) 3393.
[18] E. Cuttaz, J. Goding, C. Vallejo-Giraldo, U. Aregueta-Robles, N. Lovell, D. Ghezzi, R.A. Green, Biomater. Sci. 7 (2019) 1372.
[19] S. Baek, R.A. Green, L.A. Poole-Warren, Acta Biomater. 10 (2014) 3048.
[20] R.T. Hassarati, J.A. Goding, S. Baek, A.J. Patton, L.A. Poole-Warren, R.A. Green, J. Polym. Sci. B Polym. Phys. 52 (2014) 666.
[21] S. Wang, Q. Xu, H. Sun, Adv. Fib. Mater. 4 (2022) 324.
[22] K. Li, X. Ni, Q. Wu, C. Yuan, C. Li, D. Li, H. Chen, Y. Lv, A. Ju, Adv. Fib. Mater. 4 (2022) 631.
[23] C. Zhu, J. Wu, J. Yan, X. Liu, Adv. Fib. Mater. 5 (2023) 12.
[24] E.A. Cuttaz, C.A.R. Chapman, O. Syed, J.A. Goding, R.A. Green, Adv. Sci. 8 (2021), 2004033.
[25] C.A.R. Chapman, E.A. Cuttaz, J.A. Goding, R.A. Green, Appl. Phys. Lett. 116 (2020), https://doi.org/10.1063/1.5138587.
[26] L.v. Kayser, D.J. Lipomi, Adv. Mater. 31 (2019), 1806133.
[27] M. Berggren, G.G. Malliaras, Science 364 (2019) 233, 1979.
[28] J. Zhang, K. Zhang, F. Xu, S. Wang, Y. Qiu, Compos. B Eng. 136 (2018), https://doi.org/10.1016/j.compositesb.2017.10.037.
[29] M.G. Han, S.H. Foulger, Small 2 (2006), https://doi.org/10.1002/smll.200600135.
[30] E.A. Cuttaz, C.A.R. Chapman, J.A. Goding, C. Vallejo-Giraldo, O. Syed, R.A. Green, in: 2021 43rd Annual International Conference of the IEEE Engineering in Medicine & Biology Society, EMBC), IEEE, 2021, pp. 5872–5875.
[31] E. Cuttaz, J. Goding, C. Vallejo-Giraldo, U. Aregueta-Robles, N. Lovell, D. Ghezzi, R.A. Green, Biomater. Sci. 7 (2019), https://doi.org/10.1039/C8BM01235K.
[32] A. Rapeaux, T.G. Constandinou, Front. Neurosci. (2022) 16, https://doi.org/10.3389/fnins.2022.852166.
[33] B. Liu, H. Cang, L. Cui, H. Zhang, Int. J. Electrochem. Sci. 12 (2017) 9907.
[34] K. Dağcı, M. Alanyalıoğlu, Electroanalysis 23 (2010) n/a.
[35] A.A. Karyakin, E.E. Karyakina, H. Schmidt, Electroanalysis 11 (1999) 149.

[36] A.A. Karyakin, A.K. Strakhova, E.E. Karyakina, S.D. Varfolomeyev, A. K. Yatsimirsky, Bioelectrochem. Bioenerg. 32 (1993), https://doi.org/10.1016/0302-4598(93)80018-P.
[37] N. Elgrishi, K.J. Rountree, B.D. McCarthy, E.S. Rountree, T.T. Eisenhart, J. L. Dempsey, J. Chem. Educ. 95 (2018) 197.
[38] T. Zhou, H. Yuk, F. Hu, J. Wu, F. Tian, H. Roh, Z. Shen, G. Gu, J. Xu, B. Lu, et al., Nat. Mater. 22 (2023) 895.
[39] K. Krukiewicz, A. Kruk, R. Turczyn, Electrochim. Acta 289 (2018), https://doi.org/10.1016/j.electacta.2018.09.011.
[40] C. Boehler, M. Asplund, J. Biomed. Mater. Res. 103 (2015), https://doi.org/10.1002/jbm.a.35252.
[41] C. Mircioiu, V. Voicu, V. Anuta, A. Tudose, C. Celia, D. Paolino, M. Fresta, R. Sandulovici, I. Mircioiu, Pharmaceutics 11 (2019) 140.
[42] B. Wu, Z. Sun, J. Wu, J. Ruan, P. Zhao, K. Liu, C. Zhao, J. Sheng, T. Liang, D. Chen, Angew. Chem. Int. Ed. 60 (2021) 9284.
[43] T. Tian, J. Ruan, J. Zhang, C.-X. Zhao, D. Chen, J. Shan, J. Biomed. Nanotechnol. 18 (2022) 660.
[44] J. Ge, E. Neofytou, T. J. Cahill, R. E. Beygui, R. N. Zare, 2011, DOI 10.1021/nn203430m..
[45] Mike Driver, Coatings for Biomedical Applications, Woodhead Publishing, 2012.
[46] C.S. Kwok, P.D. Mourad, L.A. Crum, B.D. Ratner, J. Biomed. Mater. Res. 57 (2001) 151.
[47] A. E. Abelow, K. M. Persson, E. W. H. Jager, M. Berggren, I. Zharov, n.d., DOI,10.1002/mame.201200456..
[48] K. Krukiewicz, B. Bednarczyk-Cwynar, R. Turczyn, J. K. Zak (2016), https://doi.org/10.1016/j.electacta.2016.07.055.
[49] N. Paradee, A. Sirivat (2014), https://doi.org/10.1021/jp502674f.
[50] H. Yano, K. Kudo, K. Marumo, H. Okuzaki, Sci. Adv. 5 (2019), https://doi.org/10.1126/sciadv.aav9492.
[51] S. Ji, Q. Guo, Q. Yue, L. Wang, H. Wang, J. Zhao, R. Dong, J. Liu, J. Jia, Biosens. Bioelectron. 26 (2011) 2067.
[52] S.E. Sherman, S.J. Lippard, Chem. Rev. 87 (1987) 1153.
[53] K. Kano, T. Konse, N. Nishimura, T. Kubota, Bull. Chem. Soc. Jpn. 57 (1984) 2383.
[54] P. Sarathi Guin, S. Das, 2014,DOI 10.1155/2014/517371..
[55] G.M. Rao, J. Electrochem. Soc. 125 (1978) 534.
[56] C. Molinier-Jumel, B. Malfoy, J.A. Reynaud, G. Aubel-Sadron, Biochem. Biophys. Res. Commun. 84 (1978) 441.
[57] C.G. Wermuth, Drug Discov. Today 11 (2006) 348.
[58] J.O. Akindoyo, M.D.H. Beg, S. Ghazali, M.R. Islam, N. Jeyaratnam, A.R. Yuvaraj, RSC Adv. 6 (2016), 114453.
[59] C. Kleber, K. Lienkamp, J. Rühe, M. Asplund, Adv. Healthcare Mater. 8 (2019), https://doi.org/10.1002/adhm.201801488.
[60] J. Zhang, K. Zhang, F. Xu, S. Wang, Y. Qiu, 2017,DOI 10.1016/j.compositesb.2017.10.037..
[61] M. G. Han, S. H. Foulger, n.d, DOI 10.1002/smll.200600135..
[62] E.A. Cuttaz, C.A.R. Chapman, J.A. Goding, C. Vallejo-Giraldo, O. Syed, R.A. Green, in: 2021 43rd Annual International Conference of the IEEE Engineering in Medicine & Biology Society (EMBC), IEEE, 2021.